RESEARCH PROGRESS IN MECHANICAL AND MANUFACTURING ENGINEERING
e-ISSN: 2773-4765

RPMME

Vol. 7 No. 1 (2026) 376-384
https://publisher.uthm.edu.my/periodicals/index.php/rpmme

Computational Fluid Dynamics (CFD) Analysis of Electrolyte Flow Over Electroplating Surfaces with Integrated Flow Straighteners

Eng Shao Tang[1], Wan Saiful-Islam Wan Salim[1]*

[1] *Department of Mechanical Engineering, Faculty of Mechanical and Manufacturing Engineering, Universiti Tun Hussein Onn Malaysia, Parit Raja, 86400,Johor, MALAYSIA*

*Corresponding Author: wsaiful@uthm.edu.my
DOI: https://doi.org/10.30880/rpmme.2026.07.01.039

Article Info

Received: 1 January 2026
Accepted: 10 March 2026
Available online: 28 February 2026

Keywords

Electroplating, Computational Fluid Dynamics (CFD), Flow Straighteners, Flow Uniformity, Open Area Ratio

Abstract

Electroplating is a critical process in semiconductor manufacturing, where the uniformity of metal deposition is directly governed by the distribution of electrolyte flow. Non-uniform flow often leads to current density variations and coating defects; therefore, this study utilizes Computational Fluid Dynamics (CFD) to optimize the design of integrated flow straighteners within a rectangular electroplating cell. Using the Shear Stress Transport (SST) k-ω turbulence model, a parametric analysis was conducted to evaluate the hydrodynamic effects of varying blade quantities and blade thicknesses. Flow uniformity was quantified using the Coefficient of Variation (CV) of velocity magnitude across the cathode surface. The results indicated that flow uniformity is non-linearly dependent on geometric parameters, with an optimal configuration identified at 23 blades and a blade thickness of 3.25 mm, achieving a minimum CV of 0.050. Furthermore, a dimensionless design correlation based on the Open Area Ratio, $\emptyset$ was formulated, revealing a theoretical optimum ratio of approximately 0.37. This finding establishes that the balance between flow guidance and blockage is the governing factor for uniformity, providing a robust, scalable engineering protocol for designing high-precision electroplating systems.

1. Introduction

Electroplating is a critical surface finishing technique used extensively in automotive and electronic industries to enhance corrosion resistance and durability [1]. Originating in the early 19th century [2], it has become indispensable for semiconductor manufacturing, particularly for forming interconnects in integrated circuits [3]. Driven by rising industrial demand, the global electroplating market is projected to reach USD 21,131.5 million by 2032 [4].

However, achieving uniform metal deposition remains a significant challenge, largely due to non-uniform electrolyte flow over the cathode surface. Poor flow distribution leads to uneven current density, resulting in defects such as inconsistent coating thickness and roughness [5]. These issues are often exacerbated by turbulence and stagnation zones within the cell, which degrade ion transport efficiency [6].

To address these hydrodynamic problems, flow straighteners are employed to streamline electrolyte movement and suppress vortex formation [7]. The effectiveness of these devices depends heavily on geometric parameters like blade quantity. While increasing the number of blades generally improves flow alignment,

This is an open access article under the CC BY-NC-SA 4.0 license.

studies indicate that excessive blades can induce new turbulence and pressure losses, necessitating careful optimization [8].

Similarly, blade thickness plays a crucial role in flow uniformity. Research utilizing CFD optimization has shown that thicker blades increase obstruction and energy dissipation, whereas thinner blades must provide sufficient structural guidance [9]. To scale these designs effectively across different reactor sizes, dimensionless parameters such as the open area ratio are essential for predicting flow behavior [10].

This study utilizes Computational Fluid Dynamics (CFD) to investigate and optimize the integration of flow straighteners within a rectangular electroplating cell [11]. The primary objective is to evaluate the hydrodynamic effects of varying blade quantities and thicknesses on flow uniformity. By identifying the optimal configuration and formulating a dimensionless design correlation, this research aims to provide a scalable solution for high-precision electroplating applications.

2. Methodology

2.1 Numerical Simulation Overview

The hydrodynamic performance of the electroplating cell was evaluated using CFD simulations executed in ANSYS Fluent. The study utilized a structured three-stage workflow comprising pre-processing, processing, and post-processing to model the steady-state, incompressible, and single-phase turbulent flow within the reactor. A flowchart summarizing the simulation methodology is presented in Fig. 1.

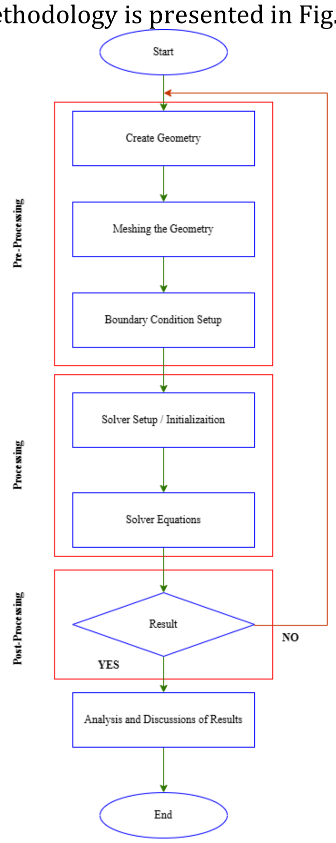

Fig. 1 *CFD Simulation Flow Chart*

2.2 Pre-Processing

A three-dimensional geometry of the rectangular electroplating cell was developed using SolidWorks, featuring chamber dimensions of 130 mm in length and 32 mm in height, with a fixed 5 mm inter-electrode gap to replicate a realistic wafer plating environment. The isometric view of the reactor geometry is illustrated in Fig. 2. To systematically assess flow conditioning, eleven distinct configurations were modelled, varying the number of straightener blades from 0 to 23 and blade thicknesses from 1.25 mm to 4.25 mm.

Penerbit UTHM

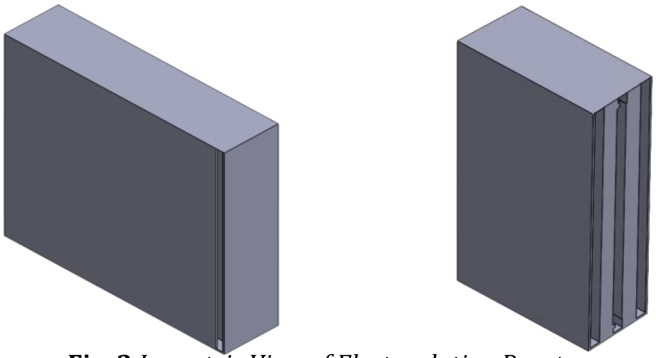

Fig. 2 *Isometric View of Electroplating Reactor*

The fluid domain was discretized using a structured mesh generated in ANSYS Meshing. A Grid Independence Test (GIT) was conducted to eliminate mesh discretization errors. Five mesh densities were evaluated by monitoring the pressure drop across the reactor. As shown in Table 1, increasing the element count from 478,335 (Mesh 1) resulted in a marginal deviation of 0.09%, indicating a mesh-independent solution. Consequently, Mesh 1 was selected for all subsequent simulations to optimize computational efficiency [12]. The mesh quality was further validated against standard metrics, achieving a maximum skewness of 0.85 and orthogonal quality above 0.15.

Table 1 *Grid Independence Test Result*

Mesh	Element Size (mm)	Number of Elements	Number of Nodes	Pressure Inlet (Pa)	Pressure Outlet (Pa)	Pressure Drop (Pa)	Deviation (%)
1	1.50	478,335	103,832	869.65	-1.14	870.79	0.09
2	1.45	520,544	112,521	868.97	-1.02	869.99	0.63
3	1.40	568,609	122,095	863.37	-1.16	864.53	0.48
4	1.35	628,453	133,761	867.46	-1.26	868.73	0.10
5	1.30	701,114	148,359	868.27	-1.31	869.58	—

2.3 Governing Equation

The simulation solves the conservation laws for mass and momentum under steady-state, incompressible conditions. The continuity equation (Eq. 1) and the momentum conservation equation (Eq. 2) are defined as:

$$\nabla \cdot \vec{v} = 0 \tag{1}$$

$$\rho\left(\frac{\partial V}{\partial t} + V \cdot \nabla \mathrm{V}\right) = -\nabla \mathrm{p} + \mu \Delta^2 V + \rho g \tag{2}$$

In the context of the Reynolds-Averaged Navier-Stokes (RANS) formulation used in this study, the viscosity term, μ represents the effective viscosity, μ_{eff} which combines molecular viscosity and turbulent viscosity. To calculate this turbulent viscosity and close the equations, the Shear Stress Transport (SST) k-ω turbulence model was employed [13].

2.4 Processing

The working fluid was defined as water at 20°C with a density of 998.21 kg/m^3 and dynamic viscosity of 1.002×10^{-3} Pa · s [14]. Boundary conditions included a velocity inlet set to 0.52 m/s, corresponding to a turbulent Reynolds number of 4,000, and a pressure outlet set to 0 Pa gauge pressure. The pressure-velocity coupling was handled using the SIMPLE algorithm, with second-order upwind schemes applied for momentum discretization to enhance precision. Convergence was determined when residuals for all governing equations fell below 10^{-4} as illustrated in the residual plot in Fig. 3.

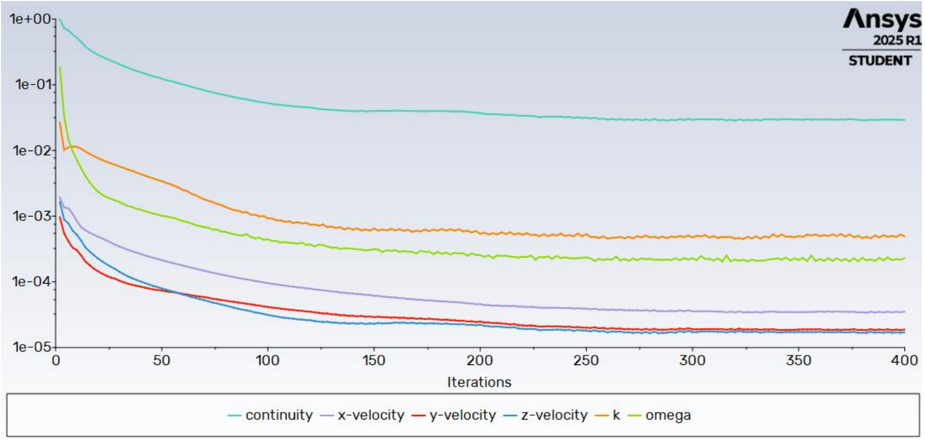

Fig. 3 *Residual Graph for Converged Solution*

2.5 Post-Processing

Post-processing focused on the quantitative statistical analysis of the flow field rather than qualitative visual inspection. To rigorously evaluate flow distribution, velocity magnitude data was extracted along a horizontal plane near the cathode surface 1. A radial sampling method was employed to quantify uniformity; as shown in Fig. 4, radial lines covering 180 degrees were defined from the center of the cathode extending to the outer edge of the plating region. The velocity data extracted along these lines was normalized using the ratio, r/R to facilitate comparative analysis across the surface.

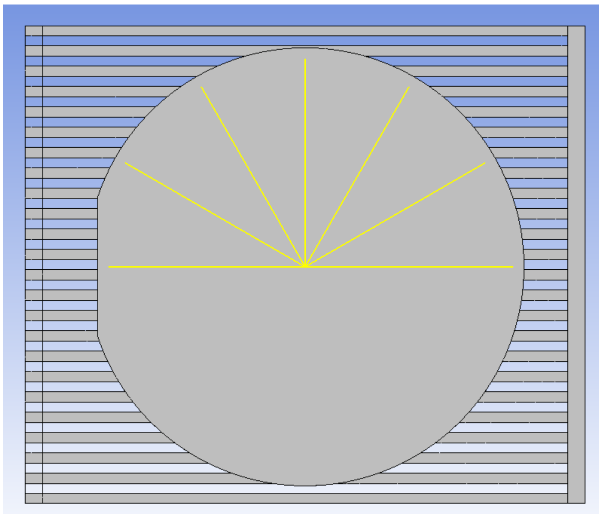

Fig. 4 *Radial Lines from the Cathode*

The primary metric for flow uniformity was the Coefficient of Variation (CV), calculated using Eq. 3. The CV normalizes the standard deviation, σ by the mean velocity, $\bar{v}$, ensuring that uniformity is assessed relative to the bulk flow speed, thus preventing misinterpretation due to blockage-induced velocity increases.

$$\mathrm{CV} = \frac{\sigma}{\bar{v}} = \frac{\sqrt{\frac{1}{N-1}\sum_{i=1}^{N}(v_i - \bar{v})^2}}{\bar{v}} \tag{3}$$

To facilitate the development of a universal design rule, geometric parameters were synthesized into a dimensionless Open Area Ratio, ∅. This parameter, defined in Eq. 4, represents the ratio of the gap size, g to the center-to-center pitch, P, allowing for the correlation of flow uniformity results against a universal geometric standard.

$$\emptyset = \frac{g}{P} = \frac{P - T}{P} \tag{4}$$

3. Results and Discussion

3.1 Parametric Analysis of Flow Straightener Geometry

To systematically evaluate the hydrodynamic performance of the flow straighteners, a parametric study was conducted by isolating key geometric variables. The primary objective was to determine how specific design modifications influence the uniformity of electrolyte flow across the cathode surface. This section examines the individual effects of two critical parameters: the number of straightener blades and the blade thickness. By analysing the velocity distribution and resulting CV for each configuration, the fundamental mechanisms governing flow alignment and blockage were identified prior to synthesizing a universal design correlation.

3.1.1 Influence of Blade Quantity

The number of straightener blades fundamentally determines flow segmentation and channel aspect ratio. To evaluate this, six configurations were simulated with blade counts ranging from 0 to 23, while maintaining a constant blade thickness of 2.25 mm. The flow uniformity was quantified using the CV of the velocity magnitude across the cathode surface, where a lower CV indicates superior uniformity. The specific CV results for each configuration are detailed in Table 2.

Table 2 *Coefficient of Variation (CV) for Different Blade Quantities*

Number of Blades	Coefficient of Variation (CV)
0 (Baseline)	0.067147
5	0.084882
10	0.073164
15	0.068123
20	0.050800
23	0.050678

As illustrated in Fig. 5 and the tabulated data, the relationship between blade count and flow uniformity is non-linear. The baseline configuration exhibited a CV of 0.067, indicating moderate non-uniformity driven by inlet jetting. Contrary to expectations, introducing a small number of blades such as 5 and 10 initially degraded performance, increasing the CV to a peak of 0.085. This phenomenon suggests that widely spaced blades act as bluff bodies, generating wake instabilities without providing sufficient channel length to realign the flow.

A transition to a uniform flow regime was observed at 15 blades, where the CV returned to baseline levels. Significant improvement occurred beyond 20 blades, with the 23-blade configuration achieving the lowest CV of 0.051. This result identifies 23 blades as the optimal quantity for this reactor geometry, providing the highest degree of flow segmentation and velocity consistency essential for high-precision wafer plating.

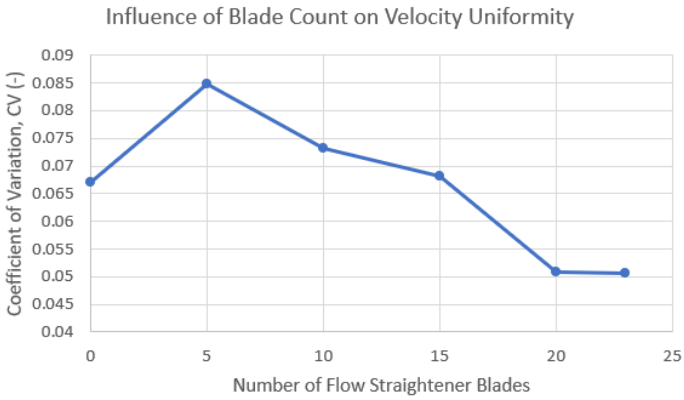

Fig. 5 *Effect of Number of Blades on Velocity Uniformity*

3.1.2 Influence of Blade Thickness

Using the optimal 23-blade configuration, the influence of blade thickness was investigated across a range of 1.25 mm to 4.25 mm. The quantitative results for flow uniformity are presented in Table 3.

Table 3 *Coefficient of Variation (CV) for Different Blade Quantities*

Blade Thickness (mm)	Coefficient of Variation (CV)
1.25	0.057349
2.25	0.050678
2.75	0.050904
3.25	0.050253
3.75	0.060698
4.25	0.055898

The results, depicted in Fig. 6, reveal a distinct parabolic trend. Thin blades which is 1.25mm yielded a relatively high CV of 0.057, likely due to insufficient physical structure to effectively guide the flow. Conversely, increasing thickness beyond 3.75 mm caused a sharp decline in uniformity due to the "blockage effect," where restricted open areas accelerate the electrolyte into high-velocity jets, creating downstream turbulence.

An intermediate thickness of 3.25 mm was identified as the optimal design point, achieving the absolute minimum CV of 0.050. This thickness provides an ideal hydrodynamic balance: it is substantial enough to enforce parallel streamlines and suppress lateral motion, yet thin enough to minimize wake formation and pressure loss.

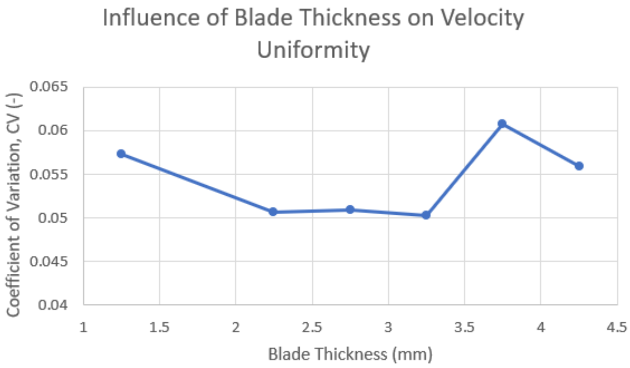

Fig. 6 *Influence of Blade Thickness on Velocity Uniformity*

3.2 Dimensionless Design Correlation

To extend the applicability of these findings to electroplating reactors of varying scales, the geometric variables were synthesized into a universal dimensionless parameter: the Open Area Ratio, Ø. This ratio represents the balance between flow guidance and blockage, calculated as Ø=g/P, where g is the gap width and P is the pitch.

When the flow uniformity data from all simulated configurations which is summarized in Table 4, is plotted against the open area ratio which is shown in Fig. 7, the results collapse onto a distinct second-order polynomial curve defined by Eq. 5:

$$y = 0.1241x^2 - 0.0918x + 0.0671 \qquad (5)$$

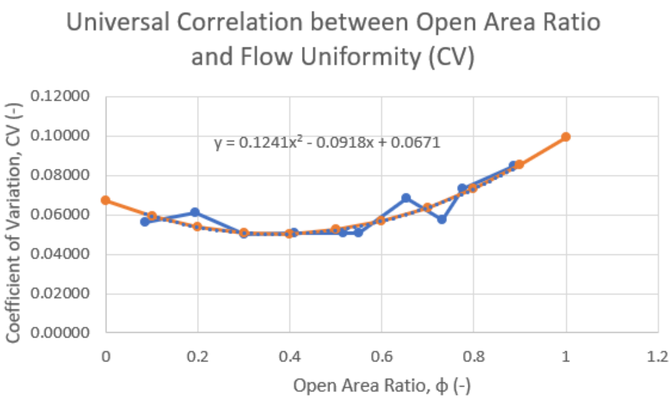

Fig. 7 *Universal Correlation between Open Area Ratio and Flow Uniformity (CV)*

The curve identifies a clear "trough" of optimal performance between ratios of 0.30 and 0.55. Mathematical optimization of the regression equation yields a theoretical optimum open area ratio of approximately $\emptyset \approx 0.37$. This finding confirms that the balance between flow guidance and blockage is the governing factor for uniformity, rather than absolute dimensions.

Table 4 *Consolidated Geometric Parameters and Flow Uniformity Results*

No.	Number of Blades	Blade Thickness, t (mm)	Pitch, P (mm)	Gap, g (mm)	Open Area Ratio, $\emptyset = \frac{g}{P}$	CV (-)
1	5	2.25	20.00	17.75	0.888	0.08488
2	10	2.25	10.00	7.75	0.775	0.07316
3	15	2.25	6.50	4.25	0.654	0.06812
4	20	2.25	5.00	2.75	0.550	0.05080
5	23	2.25	4.65	2.4	0.516	0.05068
6	23	1.25	4.65	3.4	0.731	0.05735
7	23	2.75	4.65	1.9	0.409	0.05090
8	23	3.25	4.65	1.4	0.301	0.05025
9	23	3.75	4.65	0.9	0.194	0.06070
10	23	4.25	4.65	0.4	0.086	0.05590

3.3 Universal Design Application

A key outcome of this study is the formulation of a scalable design protocol. By maintaining the optimal open area ratio of $\emptyset \approx 0.37$, the hydrodynamic benefits observed in the simulation can be replicated in reactors of varying sizes. The gap width, g for any new reactor scale can be determined using Eq. 6, where P is the pitch derived from the reactor width and selected blade count, N.

$$g = 0.37 \times P = 0.37 \times \frac{L_{new}}{N} \quad (6)$$

This scaling strategy ensures that the balance between flow guidance and blockage remains constant, effectively serving as a universal design rule for industrial electroplating systems.

3.4 Case Study: Scaling to a Large-Format Reactor

To demonstrate the practical utility of the dimensionless design correlation, a theoretical scaling scenario was analyzed for a large-scale industrial wafer plating tank with a fluid domain width, L of 300 mm. This system represents a geometry approximately 2.3 times larger than the experimental model.

The design objective was to replicate the optimal flow uniformity by targeting the universal open area ratio of $\emptyset \approx 0.37$. A blade count, N of 60 was selected to maintain a grid resolution comparable to the experimental setup4. The geometric dimensioning proceeds sequentially as follows:

First, the pitch, P is calculated based on the total width:

$$P = \frac{L}{N} = \frac{300\ mm}{60} = 5.00\ mm$$

Next, the required gap, g is determined by applying the optimal open area ratio to the pitch:

$$g = 0.37 \times P = 0.37 \times 5.00\ mm = 1.85\ mm$$

Finally, the necessary blade thickness, T is derived from the remaining solid portion of the pitch:

$$T = P - g = 5.00\ mm - 1.85\ mm = 3.15\ mm$$

By manufacturing the flow straightener with a blade thickness of 3.15 mm and a gap of 1.85 mm, the reactor is geometrically tuned to the optimal point of the uniformity curve. This approach ensures that the large-scale reactor will exhibit the minimum possible velocity deviation, effectively replicating the high-performance characteristics observed in the simulation without the need for extensive iterative testing.

4. Conclusion

This study successfully investigated the hydrodynamic optimization of a rectangular electroplating cell through the integration of flow straighteners. Using CFD simulations, the effects of blade quantity and thickness on electrolyte flow uniformity were systematically evaluated. The results demonstrate that flow uniformity is non-linearly dependent on geometric parameters. Increasing the number of blades generally improves flow alignment, with an optimal configuration identified at 23 blades, which achieved a CV of 0.051. Conversely, blade thickness exhibited a parabolic trend, where an intermediate thickness of 3.25 mm provided the ideal balance between flow guidance and blockage, yielding the lowest CV of 0.050.

A significant contribution of this work is the formulation of a dimensionless design correlation based on the Open Area Ratio, $\emptyset$. The flow uniformity data collapsed onto a distinct second-order polynomial curve, revealing a theoretical optimum open area ratio of approximately $\emptyset \approx 0.37$. This finding confirms that the balance between flow guidance and blockage is the governing factor for uniformity, irrespective of absolute reactor dimensions. Consequently, a scalable design protocol was established, enabling engineers to calculate optimal geometric parameters for reactors of any scale. This research provides a robust, data-driven framework for enhancing the efficiency and quality of high-precision electroplating processes in the semiconductor industry.

Acknowledgement

The authors would like to thank the Faculty of Mechanical and Manufacturing Engineering, Universiti Tun Hussein Onn Malaysia for its support.

Conflict of Interest

Authors declare that there is no conflict of interests regarding the publication of the paper.

Author Contribution

The authors confirm contribution to the paper as follows: ***study conception and design:*** *Eng Shao Tang, Wan Saiful-Islam Wan Salim;* ***data collection:*** *Eng Shao Tang, Wan Saiful-Islam Wan Salim;* ***analysis and interpretation of results:*** *Eng Shao Tang, Wan Saiful-Islam Wan Salim;* ***draft manuscript preparation:*** *Eng Shao Tang, Wan Saiful-Islam Wan Salim. All authors reviewed the results and approved the final version of the manuscript.*

References

[1] Gugua, E. C., Ujah, C. O., Asadu, C. O., Von Kallon, D. V., & Ekwueme, B. N. (2024). Electroplating in the modern era, improvements and challenges: A review. Hybrid Advances, 7, 100286. https://doi.org/10.1016/J.HYBADV.2024.100286

[2] Bellis, M. (2019, November 24). Electroplating: History and Timeline. ThoughtCo. https://www.thoughtco.com/history-of-electroplating-1991599

[3] Jiang, T., & Hu, H. (2025). Review of Evolution and Rising Significance of Wafer-Level Electroplating Equipment in Semiconductor Manufacturing. Electronics, 14(5). https://doi.org/10.3390/ELECTRONICS14050894

[4] Jaiswal, C. (2025, February). Electroplating Market Size, Share, Growth | Report, 2032. Market Research Future. https://www.marketresearchfuture.com/reports/electroplating-market-8130

[5] Konstantin, I. (2002). The Current Distribution in Electrochemical Cells. Fundamental Aspects of Electrometallurgy, 101–143. https://doi.org/10.1007/0-306-47564-2_4

[6] Yue, B., Zhu, G., Wang, Y., Song, J., Chang, Z., Guo, N., & Xu, M. (2021). Uncertainty analysis of factors affecting coating thickness distribution during nickel electrodeposition. Journal of Electroanalytical Chemistry, 891, 115274. https://doi.org/10.1016/J.JELECHEM.2021.115274

[7] Lyndsell, A., & Buick, J. M. (2023). An Improved Design for Flow Conditioning in Waste Water Pipes. Waste, 1(2), 414–425. https://doi.org/10.3390/WASTE1020025

[8] Zhang, X., Ge, H. E., Liu, Z., & Liu, Y. Q. (2024). Analysis of Flow Straightener on the Internal Flow Field of Three-Phase Jet Fire Monitors. International Journal of Simulation Modelling, 23(1), 101–112. https://doi.org/10.2507/IJSIMM23-1-676

[9] Xiang, Q. J., Xue, L., Kim, K. Y., & Shi, Z. F. (2019). Multi-objective optimization of a flow straightener in a large capacity firefighting water cannon. Journal of Hydrodynamics, 31(1), 137–144. https://doi.org/10.1007/s42241-019-0018-0

[10] Idel'chik, I. E. (1966). Handbook of Hydraulic Resistance.

[11] Ji, G., Zhang, M., Lu, Y., & Dong, J. (2023). The Basic Theory of CFD Governing Equations and the Numerical Solution Methods for Reactive Flows. Computational Fluid Dynamics - Recent Advances, New Perspectives and Applications. https://doi.org/10.5772/INTECHOPEN.113253

[12] Adam, N. M., Attia, O. H., Al-Sulttani, A. O., Mahmood, H. A., As'arry, A., & Rezali, K. A. M. (2020). Numerical analysis for solar panel subjected with an external force to overcome adhesive force in desert areas. *CFD Letters*, 12(9), 60-75.

[13] SimScale. (2025, April 8). *K-Omega Turbulence Models | Global Settings*. SimScale. https://www.simscale.com/docs/simulation-setup/global-settings/k-omega-sst/

[14] Evans, P. (2015, March 29). *Properties of water at atmospheric pressure*. The Engineering Mindset. https://theengineeringmindset.com/properties-of-water-atmospheric-pressure-saturated-liquid/